A mixed Fourier transform for impedance boundary conditions of acoustic waves at grazing incidence

Alexander N. Carr,[1] Joel B. Lonzaga,[2] and Steven A. E. Miller[1]

[1]Department of Mechanical and Aerospace Engineering, University of Florida, Gainesville, FL

[2]Structural Acoustics Branch, NASA Langley Research Center, Hampton, VA, United States

181st Meeting of The Acoustical Society of America

Acknowledgements

- This material is based upon work supported by the Commercial Supersonic Technology Project of the National Aeronautics and Space Administration under Grant No. 80NSSC19K1685 issued through the NASA Fellowship Activity.
- Special thanks to Will Doebler, Alexandra Loubeau, Sriram Rallabhandi and others at NASA Langley Structural Acoustics Branch for advice and guidance.

Problem

- Problem:
  - Sonic boom near lateral cutoff impacted by ground impedance
  - Incorporate ground impedance in prediction

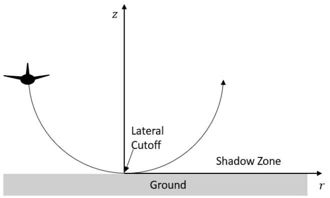

Figure 1: Illustration of lateral cutoff region

- Goals:
  - Adapt a transform method to incorporate ground impedance
  - Implement in a one-way solver with angular spectrum method
  - Discuss future implementation in acoustic propagation codes, specifically sonic boom propagation near lateral cutoff
  - Big picture: advanced prediction capabilities for flight test planning

Previous Approaches

- Start with simple problem of monopole above impedance plane
- Current methods:
  - Geometrical acoustics [1]
  - Fast-field program [2, 3]
  - Parabolic equation (and wide-angle parabolic eqn.) [4]
- Drawbacks:
  - Caustics
  - Fourier transform both source and image plane
  - Paraxial approximation [5]

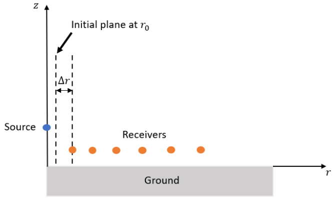

Figure 2: Diagram of sound propagation by a point source over a finite impedance plane

Approach

- Start with initial solution at initial plane r_0
- Take transform in z
- Adapt mixed Fourier transform method to account for ground boundary condition
- Compute solution of ODE on new plane $(r_0 + \Delta r)$
- Take inverse transform and repeat
- Can be incorporated into split-step marching codes (with flow effects, nonlinear distortion, etc.)

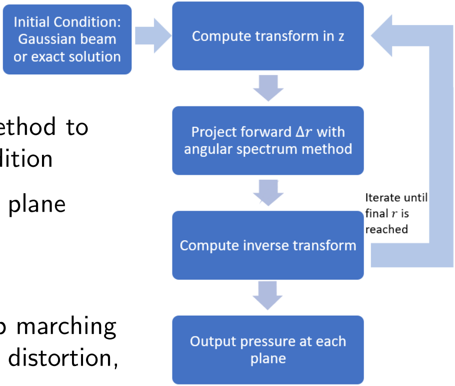

Method Outline

- Present the angular spectrum method for free space
- Discuss transforms for presence of infinite plane
- Present mixed Fourier transform approach
- Incorporate into angular spectrum method

Helical Wave Spectrum

- Start with Helmholtz equation, assume axisymmetry
- Take Fourier transform in z

$$r^2 \frac{d^2 \tilde{P}}{dr^2} + r \frac{d\tilde{P}}{dr} + (rk_r)^2 \tilde{P} = 0 \tag{1}$$

$$k_r^2 = k^2 - k_z^2 \tag{2}$$

- Spectrum at r_0 is known, compute at $r_0 + \Delta r$
- Outgoing wave solution [6] (verified by asymptotic form of $H_0^1(rk_r)$)

$$\tilde{P}(r_0 + \Delta r) = \tilde{P}(r_0) \frac{H_0^1\left((r_0 + \Delta r)k_r\right)}{H_0^1\left(r_0 k_r\right)} \tag{3}$$

- How do we incorporate boundary condition? η_g = normalized ground admittance

$$\left[\frac{\partial P}{\partial z} + ik\eta_g P\right]_{z=0} = 0 \tag{4}$$

Mixed Fourier Transform

UF UNIVERSITY of FLORIDA

- Dirchelet BC: sine transform
- Neumann BC: cosine transform
- Assume a transform that is a combination of sine and cosine

$$\tilde{P}(r, k_z) = \mathcal{N}(P) = \int_0^\infty P(r, z) \left(a \cos(k_z z) + b \sin(k_z z)\right) dz \quad (5)$$

- Integrate by parts, apply boundary condition: $a = -k_z$ and $b = \alpha$
- $\alpha = ik\eta_g$
- Inverse transform given by Kuttler and Dockery [7]

$$P(r, z) = Ke^{-\alpha z} + \frac{2}{\pi} \int_0^{-\infty} \tilde{P}(r, k_z) \frac{\alpha \sin(k_z z) - k_z \cos(k_z z)}{\alpha^2 + k_z^2} dk_z, \quad (6)$$

- When $Re(\alpha)$ approaches zero, denominator could approach a pole

Discrete Mixed Fourier Transform

UF UNIVERSITY of FLORIDA

- Instead, compute the discrete mixed Fourier transform (DMFT) [8]
- Consider the auxillary function

$$w(z) = \frac{\partial P}{\partial z} + ik\eta_g P, \tag{7}$$

- Take sine transform of $w(z)$
- Propagate forward with Eqn. 3, substitute $\tilde{w}$ for $\tilde{P}$
- Take inverse sine transform of $\tilde{w}$
- Numerically compute particular solution ψ of Eqn. 7
- P is the sum of particular and homogeneous (ϕ) solutions

$$P = \psi + \phi \tag{8}$$

- Details on procedure: [8, 9, 10]

Accuracy of Computing DMFT

UF UNIVERSITY of FLORIDA

- Numerical issues arise in MFT when $\mathrm{Re}(\eta_g) < \max(k_z)/k$
- To test accuracy of DMFT vs MFT, take a test function, say $\sin(2\pi z/h)$
- Set $\mathrm{Im}(\eta_g) = 0$ and vary $\mathrm{Re}(\eta_g)$
- Perform forward (Eqns. 5 and 11-13) and inverse (Eqns. 6 and 15-16)
- Compare error to original function
- Test functions: sine, cosine, exponential, and hyperbolic cosine all used

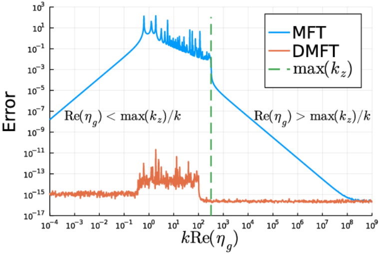

Figure 3: L^2 norm error between the original function (sine wave) and the function after applying the forward and inverse transforms of the MFT and DMFT. Note the greatly reduced error of the DMFT compared to the MFT for $k\mathrm{Re}(\eta_g) < \max(k_z)$

Benchmark Case

- Verify method with outdoor sound propagation benchmark cases [1]
- Case 1: Propagation over porous sand in medium with no refraction effects
- Ground impedance: four parameter model of Attenborough [11, 12]
- Initial condition: exact solution at $r = 1$ m

Table 1: Problem parameters for sound propagation of monopole source above a homogeneous isotropic layer of porous sand [1]

Parameter	Value
Source height (z_s)	5 m
Receiver height (z_r)	1 m
Sound speed (c_0)	343 m s^{-1}
Air Density (ρ_0)	1.2 kg m^{-3}
Flow resistivity (σ)	366000.0 Pa s m^{-2}
Porosity (Ω)	0.27
Pore shape factor (s_p)	0.5
Grain shape factor (n_p)	0.5

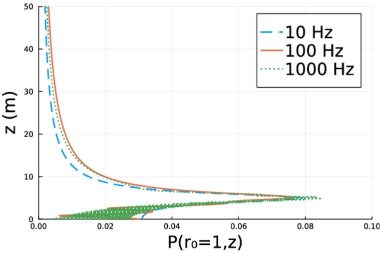

Figure 4: Initial conditions at $r_0 = 1$ m for each of the three source frequencies considered.

Transmission Loss

Table 2: Source frequencies and associated L2 norm error of predictions when compared to exact solution

Frequency	Percent Error
1 Hz	0.48 %
10 Hz	0.45 %
100 Hz	0.26 %
1000 Hz	1.06 %

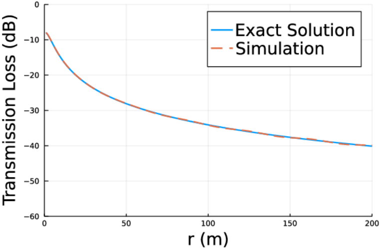

Figure 5: Transmission loss at 10 Hz.

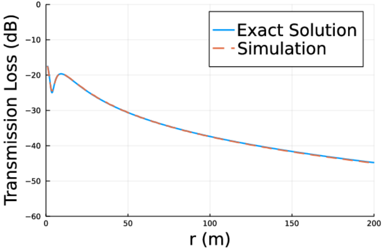

Figure 6: Transmission loss at 100 Hz.

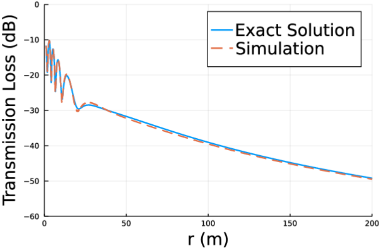

Figure 7: Transmission loss at 1000 Hz.

Summary and Conclusions

- Current progress in adapting DMFT to acoustic propagation
- Incorporated into angular spectrum method, no paraxial approximation
- Results compared to benchmark cases
- Largest error at 1000 Hz
- Future Work:
  - Ongoing work in adapting DMFT method to computational acoustics
  - Extend to 3D non-axisymmetric problems
  - Integrate with sonic boom prediction code near lateral cutoff region

UF UNIVERSITY of FLORIDA

Thank you

References I

[1] K. Attenborough, S. Taherzadeh, H. E. Bass, X. Di, R. Raspet, G. R. Becker, A. Güdesen, A. Chrestman, G. A. Daigle, A. L'Espérance, Y. Gabillet, K. E. Gilbert, Y. L. Li, M. J. White, P. Naz, J. M. Noble, and H. A. J. M. van Hoof, "Benchmark cases for outdoor sound propagation models," *The Journal of the Acoustical Society of America*, vol. 97, pp. 173–191, Jan. 1995.

[2] S. Franke and G. Swenson, "A brief tutorial on the fast field program (FFP) as applied to sound propagation in the air," *Applied Acoustics*, vol. 27, no. 3, pp. 203–215, 1989.

[3] M. West, R. Sack, and F. Walkden, "The fast field program (FFP). a second tutorial: Application to long range sound propagation in the atmosphere," *Applied Acoustics*, vol. 33, no. 3, pp. 199–228, 1991.

[4] K. E. Gilbert and X. Di, "A fast green's function method for one-way sound propagation in the atmosphere," *The Journal of the Acoustical Society of America*, vol. 94, pp. 2343–2352, Oct. 1993.

[5] V. E. Ostashev, D. K. Wilson, and M. B. Muhlestein, "Wave and extra-wide-angle parabolic equations for sound propagation in a moving atmosphere," *The Journal of the Acoustical Society of America*, vol. 147, pp. 3969–3984, June 2020.

[6] E. G. Williams, *Fourier Acoustics*.
Elsevier, 1999.

[7] J. R. Kuttler and G. D. Dockery, "Theoretical description of the parabolic approximation/fourier split-step method of representing electromagnetic propagation in the troposphere," *Radio Science*, vol. 26, no. 02, pp. 381–393, 1991.

[8] D. Dockery and J. Kuttler, "An improved impedance-boundary algorithm for fourier split-step solutions of the parabolic wave equation," *IEEE Transactions on Antennas and Propagation*, vol. 44, no. 12, pp. 1592–1599, 1996.

[9] J. R. Kuttler and R. Janaswamy, "Improved fourier transform methods for solving the parabolic wave equation," *Radio Science*, vol. 37, pp. 5–1–5–11, Mar. 2002.

[10] M. Levy, *Parabolic equation methods for electromagnetic wave propagation*.
IEE electromagnetic waves series, Institution of Electrical Engineers, 2000.

[11] K. Attenborough, "Acoustical characteristics of rigid fibrous absorbents and granular materials," *The Journal of the Acoustical Society of America*, vol. 73, pp. 785–799, Mar. 1983.

[12] K. Attenborough, "Acoustical impedance models for outdoor ground surfaces," *Journal of Sound and Vibration*, vol. 99, pp. 521–544, Apr. 1985.

Poles of Inverse MFT

- Take $\text{Im}(Z_g) = 0$, then

$$\text{Im}\left(\frac{\alpha}{\alpha^2 + k_z^2}\right) = \frac{\frac{k}{\text{Re}(Z_g)}}{k_z^2 - \left(\frac{k}{\text{Re}(Z_g)}\right)^2} \quad \text{and} \quad \text{Re}\left(\frac{k_z}{\alpha^2 + k_z^2}\right) = \frac{k_z}{k_z^2 - \left(\frac{k}{\text{Re}(Z_g)}\right)^2} \tag{9}$$

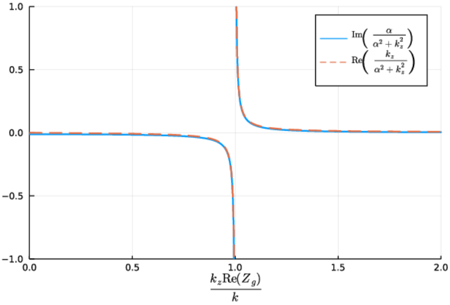

Figure 8: Poles that arise in the inverse transform

Discrete Mixed Fourier Transform

- Instead, compute the discrete mixed Fourier transform (DMFT) [8]
- Consider the auxillary function

$$w(z) = \frac{\partial P}{\partial z} + ik\eta_g P, \tag{10}$$

- $\tilde{P}$ on the interior points is just the sine transform of $w(z)$
- Forward transform:

$$\tilde{w}_1 = D \sum_{n=1}^{N} \lambda^{n-1} P_n \tag{11}$$

$$\tilde{w}_j = \mathcal{F}_s(P_n), \quad n, j = 2, \ldots, N-1 \tag{12}$$

$$\tilde{w}_N = D \sum_{n=1}^{N} (-\lambda)^{N-n} P_n \tag{13}$$

$$D = \frac{2(1-\lambda^2)}{(1+\lambda^2)(1-\lambda^{2N})} \tag{14}$$

Discrete Mixed Fourier Transform

- Inverse transform, particular solution:

$$\frac{\psi_{j+1} - \psi_{j-1}}{2\Delta z} + \alpha\psi_j = \mathcal{F}_s(\tilde{w}_n), \quad n, j = 2, \ldots, N-1 \tag{15}$$

- Homogeneous solution:

$$\phi_j = B_1\lambda^j + B_2(-\lambda)^{N-j}, \quad j = 1, \ldots, N \tag{16}$$

$$\lambda^2 + 2\alpha dz\lambda - 1 = 0 \tag{17}$$

$$B_1 = \tilde{w}_1 - D\sum_{n=1}^{N}\psi_n\lambda^n \tag{18}$$

$$B_2 = \tilde{w}_N - D\sum_{n=1}^{N}\psi_n(-\lambda)^{N-n} \tag{19}$$

- More info on DMFT in [8, 10], inverse transform is

$$P_j = \psi_j + \phi_j, \quad j = 1, \ldots, N \tag{20}$$

Transmission Loss

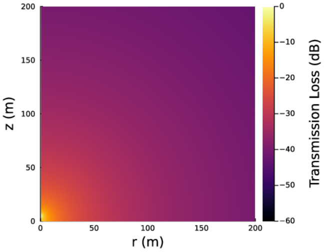

Figure 9: Exact transmission loss at 1 Hz.

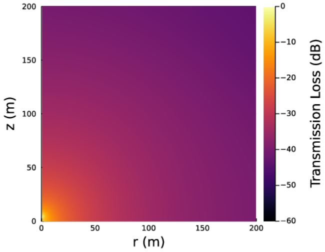

Figure 10: Predicted transmission loss at 1 Hz.

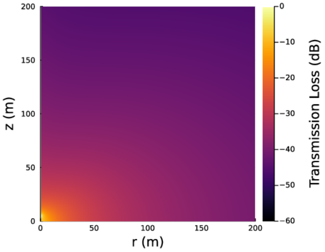

Figure 11: Exact transmission loss at 10 Hz.

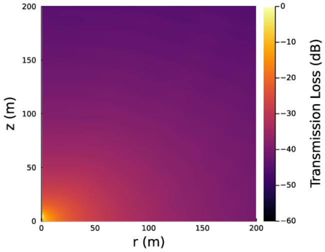

Figure 12: Predicted transmission loss at 10 Hz.

Transmission Loss

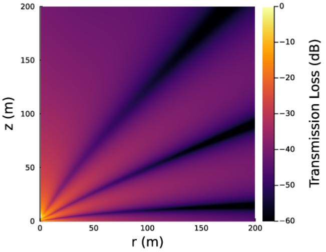

Figure 13: Exact transmission loss at 100 Hz.

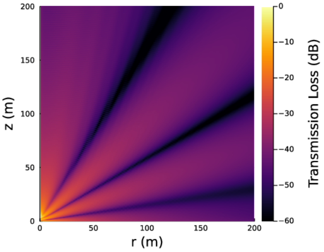

Figure 14: Predicted transmission loss at 100 Hz.

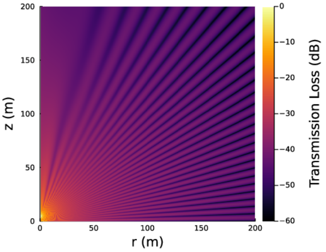

Figure 15: Exact transmission loss at 1000 Hz.

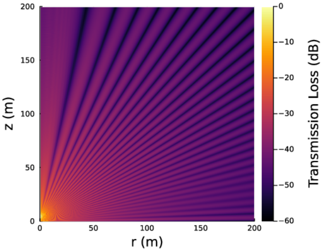

Figure 16: Predicted transmission loss at 1000 Hz.

Grid Resolution

- Simulations for higher source frequencies had less points per wavelength

Table 3: Points per wavelength in the transverse direction rounded down to nearest integer

Frequency	Points per wavelength
10 Hz	94
100 Hz	29
1000 Hz	15